Ferromagnetic quantum criticality in $Sm_{1-x}La_xNiC_2$ (x = 0.85, 0.92, and 0.96)

Wonjun Lee,[*] S. Lee, and K.-Y. Choi[†]
Department of Physics, Chung-Ang University, Seoul 06974, Republic of Korea

K.-J. Lee, B.-J. Kim, and B. J. Suh
Department of Physics, The Catholic University of Korea, Bucheon 14662, Korea

S. Shin and T. Park[‡]
Center for Quantum Materials and Superconductivity (CQMS) and Department of Physics, Sungkyunkwan University, Suwon 16419, South Korea

(Received 18 October 2017; revised manuscript received 15 December 2017; published 29 December 2017)

We report μSR experiments on the ternary compounds $Sm_{1-x}La_xNiC_2$ ($x = 0.85$, 0.92, and 0.96), crossing from a ferromagnetic to a superconducting phase. Zero-field μSR measurements of the ferromagnetic sample ($x = 0.85$) unveil a glassylike character of the ferromagnetically ordered state. At the putative quantum critical compound ($x = 0.92$), fluctuations of the Sm moments slow down below 2 K and remain dynamic down to 30 mK, showing persisting spin dynamics. Moreover, we find a time-field scaling (t/H^γ) of the μSR asymmetry function, evidencing quantum critical fluctuations. As to the superconducting material ($x = 0.96$), the muon spin-relaxation rate displays a λ-like peak at $T = 250$ mK, indicating the coexistence of weak magnetism and filamentary superconductivity. Our results demonstrate that $Sm_{1-x}La_xNiC_2$ constitutes a model system for studying a ferromagnetic quantum critical point tuned by chemical pressure.

DOI: 10.1103/PhysRevB.96.224433

I. INTRODUCTION

Intermetallic compounds offer a rich reservoir to explore quantum critical points (QCPs) since their ground states can be tuned readily by nonthermal control parameters such as magnetic field, pressure, or chemical composition. At a QCP, quantum fluctuations can give rise to unconventional superconductivity. Although antiferromagnetic QCPs have been extensively studied, not much is known about ferromagnetic QCPs due to the scarcity of relevant materials. Key materials reported to date are uranium-based heavy fermions including UGe_2 [1–3], UCoGe [3–6], URhGe [3,7], and UIr [8], which show the vanishing of superconductivity at the first-order ferromagnetic QCP except for the UCoGe compound.

Recently, the ternary rare-earth nickel carbides $Sm_{1-x}La_xNiC_2$ [9] have been reported as a promising candidate for a ferromagnetic QCP. Unlike the uranium-based heavy fermions, $Sm_{1-x}La_xNiC_2$ does not involve the complications of high pressure as the end members of this family ($SmNiC_2$ and $LaNiC_2$) are continuously varied through chemical substitution. These compounds crystallize in the noncentrosymmetric orthorhombic $CeNiC_2$-type structure ($Amm2$), as sketched in Fig. 1(a) [10]. In this family, Ni and R (= rare earth) metal ions form chains along the a axis, constituting a quasi-one-dimensional electronic structure and, thereby stabilizing a charge-density wave (CDW) state due to the Fermi surface nesting. Noteworthy is that $SmNiC_2$ and $LaNiC_2$ exhibit a ferromagnetic and a superconducting ground state, respectively, distinct from those of other $RNiC_2$ compounds [10–14].

In Fig. 1(b), we present the $T-x$ phase diagram of $Sm_{1-x}La_xNiC_2$ taken from Ref. [9]. $SmNiC_2$ undergoes a CDW transition at $T_{CDW} = 148$ K and, subsequently, a ferromagnetic transition at $T_C = 17.7$ K [13–22]. With increasing La content, the CDW phase vanishes at around $x = 0.3$, while the ferromagnetic phase persists up to $x = 0.86$. The nonmagnetic end member $LaNiC_2$ becomes a superconductor below $T_{SC} = 2.7$ K [23–25]. There are contradicting signatures for a conventional Bardeen-Cooper-Schrieffer-type versus unconventional superconductivity [24–28]. It turns out that a few percentages of Sm substitution suppresses the superconducting state. As a result, the ferromagnetic QCP is anticipated at the putative critical concentration $x_c \approx 0.92$, rendering $Sm_{1-x}La_xNiC_2$ a model system amenable to address the competition and/or coexistence of ferromagnetism and superconductivity.

Quite often, the ferromagnetic QCP is masked either by a change of its phase-transition character to first order or by an occurrence of intervening symmetry-broken states without being continuously suppressed all the way down to the expected QCP. As to $Sm_{1-x}La_xNiC_2$, the ferromagnetic transition becomes a weakly first order for a high value of x [9]. The related question is the fate of ferromagnetic order, when approaching the putative ferromagnetic QCP. μSR is a choice of experimental tools because it can distinguish between static internal magnetic field arising from a ferromagnetic phase and dynamically fluctuating field associated with a quantum disordered phase, as well as spatial inhomogeneities.

In this paper, we report a systematic μSR investigation on the ferromagnetism-superconductivity crossover in $Sm_{1-x}La_xNiC_2$ ($x = 0.85$, 0.92, and 0.96). We provide an experimental signature of the quantum phase transition from a spin-glasslike ferromagnetic state ($x = 0.85$) to a filamentary superconductivity ($x = 0.96$) coexisting with weak magnetic order. In the putative quantum critical compound ($x = 0.92$),

[*]wonjunleecau@gmail.com
[†]kchoi@cau.ac.kr
[‡]tp8701@skku.edu

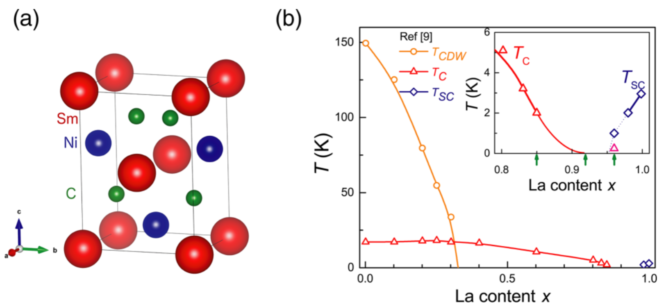

FIG. 1. (a) Crystal structure of $SmNiC_2$. The red (blue) balls depict Sm (Ni) atoms and the green balls are carbon atoms. (b) Temperature-composition phase diagram of $Sm_{1-x}La_xNiC_2$. The inset is a zoom of the phase diagram close to a putative quantum critical point at $x = 0.92$. The open triangles correspond to the ferromagnetic transition temperatures (determined by the peak of the muon spin-relaxation rate) and the open diamonds are the superconducting transition temperatures (taken from Ref. [9]). The vertical arrows mark the compositions where μSR measurements were performed.

we find evidence for a time-field scaling (t/H^{γ}) and persistent spin dynamics, indicating slow spin dynamics due to quantum critical fluctuations.

II. EXPERIMENTAL DETAILS

$Sm_{1-x}La_xNiC_2$ samples were synthesized by the arc-melting technique as described in Ref. [9]. μSR measurements were performed at the M15 and M20 beamlines in TRIUMF (Vancouver BC, Canada). For low-temperature measurements ($T = 30$ mK $- 4$ K), the samples were packed in a Ag foil packet and fixed by thermal grease on the silver holder of a dilution refrigerator in the M15 facility. High-temperature measurements ($T = 1.6 - 125$ K) were undertaken in the M20 facility equipped with a variable temperature insert. The samples were held by a Ag foil packet and thin Al-mylar tape. Zero- and longitudinal-field μSR spectra were collected to determine magnetic phases of the samples. All of the data were analyzed by using the musrfit software package [29].

III. RESULTS AND DISCUSSION

Figure 2(a) shows the zero-field (ZF)-μSR asymmetry of the $x = 0.85$ sample at selected temperatures. At high-temperature regime, the muons relax very slowly with the Gaussian-like relaxation function, which results from a combination of nuclear moments and fast fluctuating electron spins in the paramagnetic limit. As the temperature is lowered below $T = 5$ K, the muon spins display a rapid relaxation. We could not detect a coherent oscillation and a noticeable loss of the initial polarization although the macroscopic magnetic susceptibility shows a steep increase [see Fig. 3(b)]. This clearly rules out a long-range static magnetic order with well-defined internal fields. Rather, the fast decaying signal is either due to a broadening of the dynamic field distribution or the slowing down of fluctuations.

The ZF-μSR spectra were fitted using the stretched exponential relaxation function

$$a_0 P_z(t) = \exp[-(\lambda t)^{\beta}]. \tag{1}$$

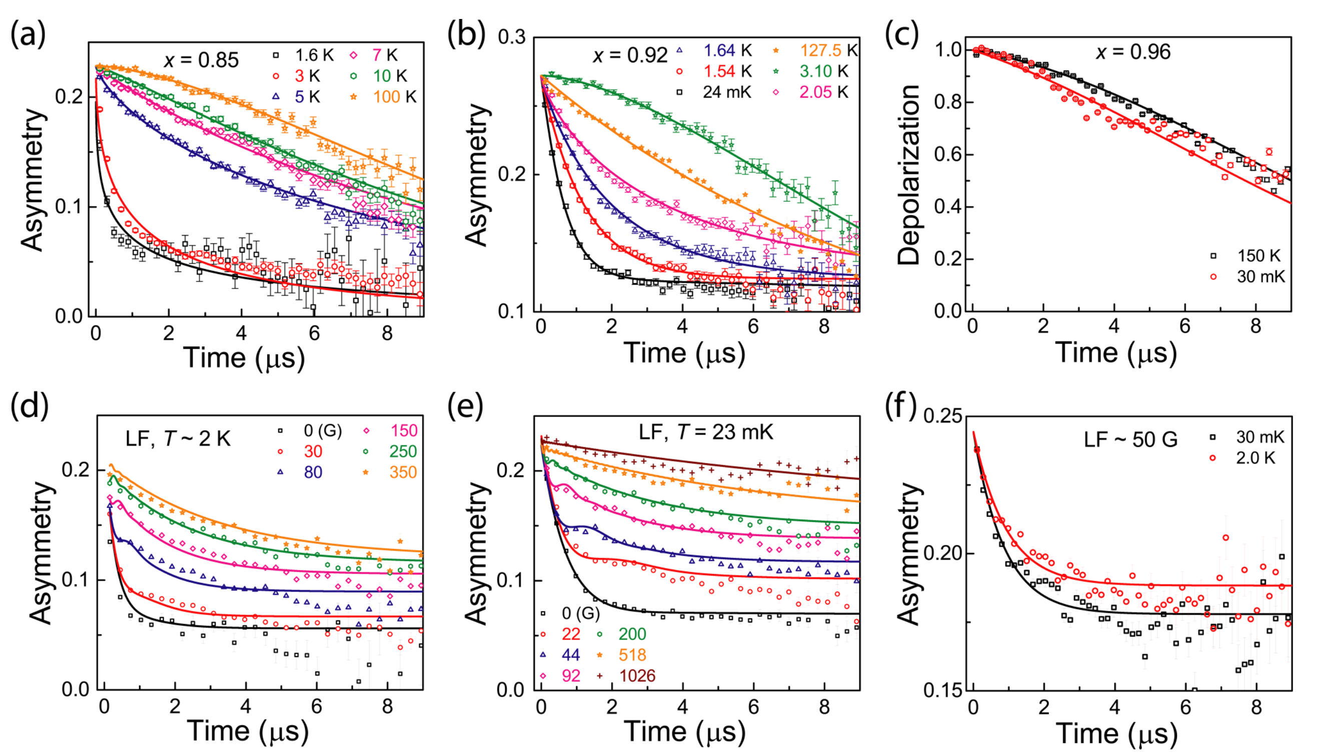

FIG. 2. Representative temperature dependence of ZF-μSR asymmetry spectra for (a) $x = 0.85$, (b) $x = 0.92$, and (c) $x = 0.96$. Longitudinal-field dependence of μSR asymmetries for (d) $x = 0.85$ measured at $T \sim 2$ K and (e) $x = 0.92$ measured at $T = 23$ mK. (f) Temperature dependence of μSR asymmetries in an applied magnetic field $B_{LF} \sim 50$ G.

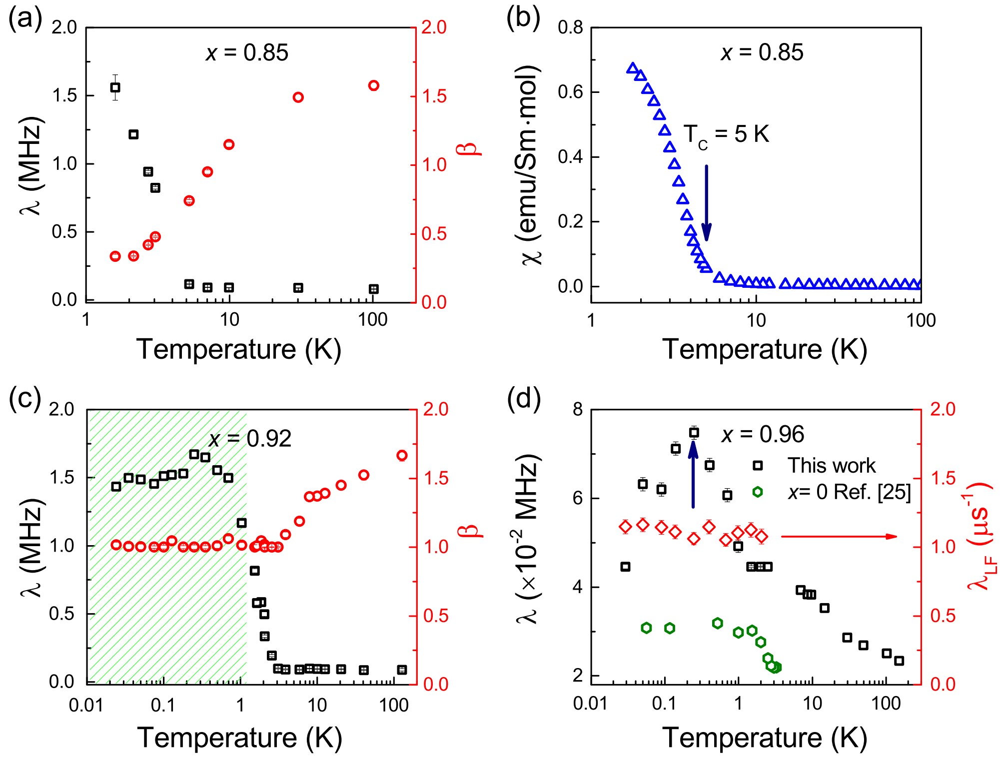

FIG. 3. (a) Temperature dependence of the muon-spin relaxation rate λ and the stretching exponent β for $x = 0.85$. (b) Temperature dependence of the static magnetic susceptibility for $x = 0.85$. (c) Temperature dependence of $\lambda(T)$ and $\beta(T)$ for $x = 0.92$. (d) Temperature dependence of $\lambda(T)$ in zero field (open squares) and in longitudinal field of $B_{LF} \approx 40$ G (open diamonds) for $x = 0.96$. For comparison, $\lambda(T)$ of $LaNiC_2$ is plotted together, taken from Ref. [25].

Here a_0 is the initial asymmetry from the sample, λ is the muon relaxation rate, and β is the stretching exponent. Fits of the asymmetry data with Eq. (1) enable us to extract λ and β. The resulting fit parameters are plotted as a function of temperature in Fig. 3(a). Below 5 K, $\lambda(T)$ steeply increases. This temperature coincides with the onset temperature of the sharply increasing magnetic susceptibility. As the temperature is further lowered below $T < 2$ K, $\beta \sim 1.6$ at high temperatures approaches toward $\beta = 0.33$. The $\beta = 1/3$ exponent is what is expected for a canonical spin glass [30,31]. Thus, our μSR data give evidence for spatially inhomogeneous frozen spins in the $x = 0.85$ compound.

We turn next to the asymmetry of ZF-μSR spectra for $x = 0.92$ measured down to 23 mK. As shown in Fig 2(b), both the $x = 0.92$ and 0.85 samples exhibit a qualitatively similar behavior, demonstrating no sign of long-range magnetic order. The ZF-μSR spectra of $x = 0.92$ are described by the stretched-exponential function

$$a_0 P_z(t) = (1 - f_{bg}) \exp[-(\lambda t)^{\beta}] + f_{bg}. \tag{2}$$

Here, the constant term f_{bg} is added to quantify the background present in the dilution refrigerator. The value of f_{bg} was taken from the $T = 23$ mK spectrum and kept constant for all temperatures. Fits of the ZF data to Eq. (2) yield the relaxation rate λ and the stretching exponent β as plotted in Fig. 3(c). At temperatures above 3 K, electron spins are in a fast fluctuating state. On cooling, $\lambda(T)$ steeply increases, indicative of a slowing down of spin correlations, and then shows a temperature-independent plateau below 0.8 K. Such a relaxation plateau has often been observed in quantum spin liquid candidates and weakly symmetry-broken states [32,33]. Noticeably, with decreasing temperature the exponent $\beta \sim 1.7$ decreases towards $\beta \sim 1$ below 3 K. It is striking that the $x = 0.92$ sample possesses a single spin-spin autocorrelation time (inferred from $\beta = 1$) unlike the $x = 0.85$ sample in spite of randomness and disorders. The simple exponential relaxation together with the persistent spin dynamics suggests that the $x = 0.92$ sample enters into a peculiar regime where spin dynamics is purely dynamic and dictated by unconventional low-energy excitations.

With a view to discriminate between the dynamic or static character of internal magnetic fields experienced by the muon, we have further performed LF-μSR measurements. Figures 2(d) and 2(e) show the evolution of the muon polarization of $x = 0.85$ and 0.92 with increasing longitudinal field. At short times, the fast relaxing component associated with nuclear moments and weak spin freezing is fully decoupled with a fairly small magnetic field of 50 G, whereas, at long times, the slow relaxing component linked to dynamic magnetic fluctuations is not completely decoupled up to $\sim$1000 G. Our LF-μSR results suggest that the fast fluctuating spins are mixed up with the frozen spins.

For the fast fluctuating fields, the decoupling relaxation rate λ_{LF} as a function of longitudinal field B_{LF} is given by the Redfield formula

$$\lambda_{LF} = \frac{1}{T_1} = \frac{2\gamma_\mu^2 \langle B_{loc}^2 \rangle \tau_c}{1 + \gamma_\mu^2 B_{LF}^2 \tau_c^2}, \tag{3}$$

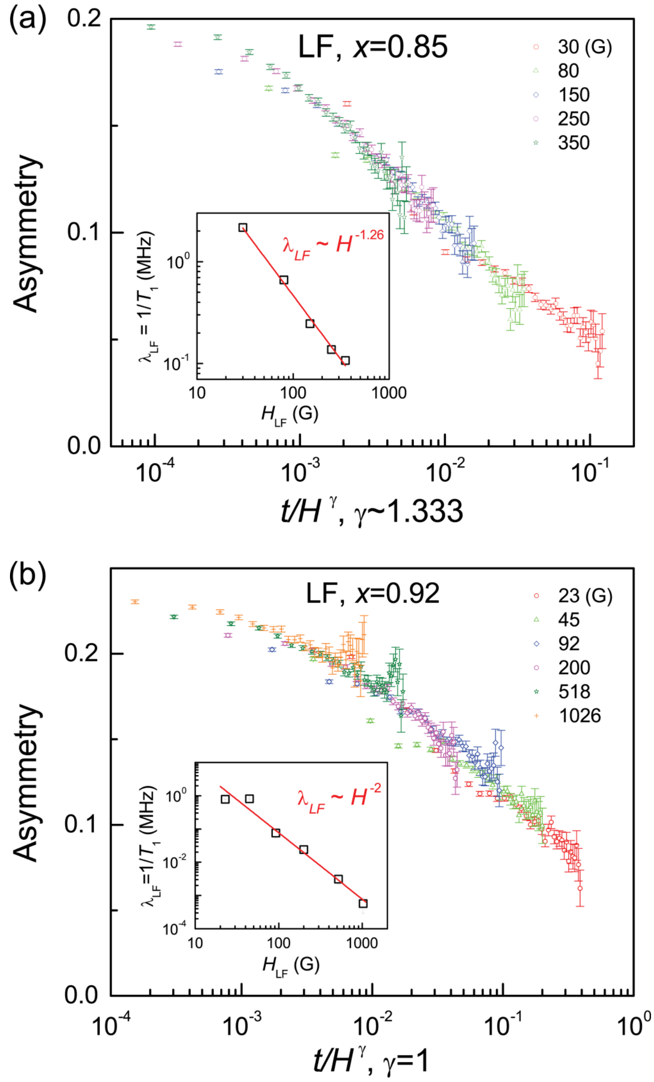

FIG. 4. Time-field scaling of LF-μSR asymmetries in log-normal scale (a) for $x = 0.85$ at $T = 2$ K and (b) for $x = 0.92$ at $T = 23$ mK. (b) The inset shows a longitudinal magnetic field dependence of the muon spin-relaxation rate on a log-log scale. The exponents are extracted by linear fits of the data plotted in log-log scale.

where τ_c is the field-independent correlation time and $\langle B_{\rm loc}^2\rangle$ is the time average of the second moment of the time-varying local field at muon sites. The H dependence of the electronic relaxation is shown in the inset of Fig. 4. For $x = 0.92$, the H dependence of $\lambda_{\rm LF}$ is fitted using a single characteristic fluctuation time $\tau_c \approx 3.4$ μs and $\gamma_\mu\langle B_{\rm loc}\rangle = \Delta \approx 0.43 - 0.55$ MHz. A rather long fluctuation time indicates slow spin dynamics in the vicinity of a QCP. We find that the LF relaxation rate follows the power law $\lambda_{\rm LF} \sim H^{-2}$, which is expected in the limit of $\gamma_\mu^2 B_{\rm LF}^2 \tau_c^2 \gg 1$ (see the inset of Fig 4). For $x = 0.85$, $\lambda_{\rm LF}$ displays the $H^{-1.26}$ dependence.

We recall that the relaxation at long times probes the spin-fluctuation dynamics and, in absence of cross-correlations, the relaxation rate is given by the Fourier transform of the dynamic spin-spin autocorrelation function, $q(t) = \langle \mathbf{S}(0)\cdot\mathbf{S}(t)\rangle$. The Fourier transform of the autocorrelation function results then in a time-field scaling relation of the μSR asymmetry, $\overline{G}(t,H) = \overline{G}(t/H^\gamma)$ [34–39]. Significantly, the exponent γ obtained from the time-field scaling relation provides information about the nature of the dynamic component of the relaxation: power-law correlation $q(t) \sim ct^{-\alpha}$ for $\gamma = 1 - \alpha < 1$ and stretched-exponential correlation $q(t) \sim \exp[-(\lambda t)^\beta]$ for $\gamma = 1 + \beta > 1$ [34].

In Fig. 4, we display the time-dependent asymmetry versus t/H^γ plot of the H-dependent LF-μSR data at $T = 2$ K for $x = 0.85$ and $T = 23$ mK for $x = 0.92$. The LF muon asymmetries of $x = 0.85$ overlap over one order of magnitude in t/H^γ with a value of $\gamma = 4/3$. This is fully consistent with the stretched spin-spin correlation with $\beta = 1/3$, determined from the ZF-μSR data. Noticeably, the critical exponents of $\alpha = 0, \beta = 1/3$, and $\gamma = 4/3$, satisfying the relation $\alpha + 2\beta + \gamma = 2$, is what is expected for the XY spin model. The putative QCP compound $x = 0.92$ shows the time-field scaling for $\gamma = 1$ over two orders of magnitude, indicating the critical slowing down of spin fluctuations expected in a quantum critical regime. We note that the ferromagnetic QCP system $CePd_{0.15}Rh_{0.85}$ displays a scaling with a similar value of $\gamma = 1.0(1)$ [37]. Taken the persistent spin dynamics and the time-field scaling with $\gamma = 1$ together, we conclude that the $x = 0.92$ compound lies in the proximity to the ferromagnetic QCP.

Finally, we discuss the ZF-μSR depolarization of $x = 0.96$, shown in Fig. 2(c). The absence of any oscillatory component confirms that there are no ordered magnetic moments. In this case, muon-spin relaxation in zero field is given by the Gaussian Kubo-Toyabe relaxation function $\Delta_{\rm KT}$ due to static, randomly oriented local fields associated with the nuclear moments at the muon site [40]. The ZF-μSR spectra are well described by $\Delta_{\rm KT}$ multiplied by a simple exponential function with electronic relaxation rate λ,

$$P_z(t) = (1 - f_{\rm bg})\Delta_{\rm KT}e^{-\lambda t} + f_{\rm bg}e^{-\lambda_{\rm bg}t}$$
$$\Delta_{\rm KT}(t) = \frac{1}{3} + \frac{2}{3}(1 - \sigma^2 t^2)\exp\left(-\frac{1}{2}\sigma^2 t^2\right). \qquad (4)$$

Here we remark that the width of Gaussian field distribution $\sigma = 0.0755$ MHz is temperature independent and is comparable to $\sigma = 0.08$ MHz of $LaNiC_2$ [25]. Furthermore, $f_{\rm bg}$ turns out to be independent of temperature and, thus, its value was kept fixed for all temperatures. As shown in Fig. 3(d), we find the substantial electronic relaxation rate λ in the superconducting state, which increases continuously down to $T_{\rm C}^{\rm onset} = 250$ mK, forming a λ-like anomaly. This is in sharp contrast to $LaNiC_2$, which shows a temperature-independent behavior below $T_{\rm SC} \sim 2.5$ K. This suggests that some fraction of the $x = 0.96$ sample has weak static magnetism on the μSR time window. From this, we infer a microscopic coexistence of magnetism and filamentary superconductivity as frequently reported in the Fe-based superconductors [41–46].

To get rid of contributions from nuclear magnetic fields, we carried out the LF-μSR measurements in an applied field of $B_{\rm LF} \approx 40$ G. The representative spectra are displayed in Fig. 2(f). The data were fitted by the Kubo-Toyabe function with a simple exponential form

$$P_{\rm LF}(t) = (1 - f_{\rm dc})\Delta_{KT}e^{-\lambda_{\rm LF}t} + f_{\rm dc}, \qquad (5)$$

where f_{dc} is introduced to account for the frozen fraction of the nuclear fields under a longitudinal field. As shown in Fig. 3(d), with decreasing temperature below 2 K, λ_{LF} is temperature independent with a value of 1.1 MHz, which is significantly larger than $\lambda \approx 0.03$ MHz in $LaNiC_2$ [25]. This lends further support to the presence of intrinsic electronic magnetic fluctuations in the superconducting state upon introducing several percentage of the Sm atoms.

Lastly, we turn to the $T - x$ phase diagram in the vicinity of the ferromagnetic QCP by adding a few data points obtained by the μSR data as shown in the inset of Fig 1(b). The phase boundary seems to have a tail towards the superconducting phase, indicating the existence of a quantum Griffith phase [47]. Further studies are needed to elucidate the quantum Griffith phase between the ferromagnetic and the superconducting phase.

IV. SUMMARY

To summarize, we have investigated the spin dynamics of $Sm_{1-x}La_xNiC_2$ ($x = 0.85$, 0.92, and 0.96) using μSR technique towards clarifying a ferromagnetic QCP. In the $x = 0.85$ compound, our ZF-μSR study unveils a spin-glass ground state. In the putative QCP sample ($x = 0.92$), we find signatures of a slowing of dynamic spin fluctuations due to a quantum criticality, evident from persistent spin dynamics and universal quantum critical scaling in t/H^{γ}. The superconducting $x = 0.96$ sample displays appreciable spin dynamics arising from electronic magnetic moments, indicating a microscopic coexistence of magnetic and superconducting states. Thus, $Sm_{1-x}La_xNiC_2$ emerges as a much-sought-after model compound for exploring a ferromagnetic quantum critical point at zero field and ambient pressure.

ACKNOWLEDGMENTS

We would like to thank B. Hitti for his assistance with μSR experiments. This work was supported by Korea Research Foundation (KRF) Grants No. 2017012642 and No. 2017-0675 and Grant No. 2012R1A3A2048816 funded by the Korea government (MEST) and by the Korean Ministry of Science, ICT, and Planning.

[1] V. Taufour, D. Aoki, G. Knebel, and J. Flouquet, Phys. Rev. Lett. **105**, 217201 (2010).
[2] S. Sakarya, P. C. M. Gubbens, A. Yaouanc, P. Dalmas de Réotier, D. Andreica, A. Amato, U. Zimmermann, N. H. van Dijk, E. Brück, Y. Huang, and T. Gortenmulder, Phys. Rev. B **81**, 024429 (2010).
[3] D. Aoki and J. Flouquet, J. Phys. Soc. Jpn. **83**, 061011 (2014).
[4] E. Slooten, T. Naka, A. Gasparini, Y. K. Huang, and A. de Visser, Phys. Rev. Lett. **103**, 097003 (2009).
[5] A. Gasparini, Y. K. Huang, N. T. Huy, J. C. P. Klaasse, T. Naka, E. Slooten, and A. de Visser, J. Low. Temp. Phys. **161**, 134 (2010).
[6] A. de Visser, N. T. Huy, A. Gasparini, D. E. de Nijs, D. Andreica, C. Baines, and A. Amato, Phys. Rev. Lett. **102**, 167003 (2009).
[7] A. Miyake, D. Aoki, and J. Flouquet, J. Phys. Soc. Jpn. **78**, 063703 (2009).
[8] T. C. Kobayashi, A. Hori, S. Fukushima, H. Hidaka, H. Kotegawa, T. Akazawa, K. Takeda, Y. Ohishi, and E. Yamamoto, J. Phys. Soc. Jpn. **76**, 051007 (2007).
[9] G. Prathiba, I. Kim, S. Shin, J. Strychalska, T. Klimczuk, and T. Park, Sci. Rep. **6**, 26530 (2016).
[10] O. I. Bodak and E. P. Marusin, Dokl. Akad. Nauk Ukr. S.S.R. Ser. A **12**, 1048 (1979).
[11] W. Schäfer, G. Will, J. K. Yakinthos, and P. A. Kotsanidis, J. Alloys Compd. **180**, 251 (1992).
[12] K. Motoya, K. Nakaguchi, N. Kayama, K. Inari, J. Akimitsu, K. Izawa, and T. Fujita, J. Phys. Soc. Jpn. **66**, 1124 (1997).
[13] H. Onodera, Y. Koshikawa, and M. Kosaka, J. Magn. Magn. Mater. **182**, 161 (1998).
[14] M. Murase, A. Tobo, H. Onodera, Y. Hirano, T. Hosaka, S. Shimomura, and N. Wakabayashi, J. Phys. Soc. Jpn. **73**, 2790 (2004).
[15] S. Shimomura, C. Hayashi, G. Asaka, N. Wakabayashi, M. Mizumaki, and H. Onodera, Phys. Rev. Lett. **102**, 076404 (2009).
[16] A. Wölfel, Liang Li, Susumu Shimomura, Hideya Onodera, and Sander van Smaalen, Phys. Rev. B **82**, 054120 (2010).
[17] J. Laverock, T. D. Haynes, C. Utfeld, and S. B. Dugdale, Phys. Rev. B **80**, 125111 (2009).
[18] T. Sato, S. Souma, K. Nakayama, T. Takahashi, S. Shimomura, and H. Onodera, J. Phys. Soc. Jpn. **79**, 044707 (2010).
[19] N. Hanasaki, Y. Nogami, M. Kakinuma, S. Shimomura, M. Kosaka, and H. Onodera, Phys. Rev. B **85**, 092402 (2012).
[20] J. H. Kim, J. S. Rhyee, and Y. S. Kwon, Phys. Rev. B **86**, 235101 (2012).
[21] B. Woo, S. Seo, E. Park, J. H. Kim, D. Jang, T. Park, H. Lee, F. Ronning, J. D. Thompson, V. A. Sidorov, and Y. S. Kwon, Phys. Rev. B **87**, 125121 (2013).
[22] D. Ahmad, Byeon Hun Min, Gyeon Im Min, Shin-Ichi Kimura, Jungpil Seo, and Yong Seung Kwon, Phys. Status Solidi B **252**, 2662 (2015).
[23] W. H. Lee, H. K. Zeng, Y. D. Yao, and Y. Y. Chen, Physica C **266**, 138 (1996).
[24] A. Sumiyama, D. Kawakatsu, J. Gouchi, A. Yamaguchi, G. Motoyama, Y. Hirose, R. Settai, and Y. Ōnuki, J. Phys. Soc. Jpn. **84**, 013702 (2015).
[25] A. D. Hillier, J. Quintanilla, and R. Cywinski, Phys. Rev. Lett. **102**, 117007 (2009).
[26] S. Katano, K. Shibata, Kotaro Nakashima, and Y. Matsubara, Phys. Rev. B **95**, 144502 (2017).
[27] Y. Iwamoto, Y. Iwasaki, K. Ueda, and T. Kohara, Phys. Lett. A **250**, 439 (1998).
[28] J. Chen, L. Jiao, J. L. Zhang, Y. Chen, L. Yang, M. Nicklas, F. Steglich, and H. Q. Yuan, New J. Phys. **15**, 053005 (2013).
[29] A. Suter and B. M. Wojek, Phys. Procedia **30**, 69 (2012).
[30] K. Binder and A. P. Young, Rev. Mod. Phys. **58**, 801 (1986).
[31] I. A. Campbell, A. Amato, F. N. Gygax, D. Herlach, A. Schenck, R. Cywinski, and S. H. Kilcoyne, Phys. Rev. Lett. **72**, 1291 (1994).

[32] P. Mendels, F. Bert, M. A. de Vries, A. Olariu, A. Harrison, F. Duc, J. C. Trombe, J. S. Lord, A. Amato, and C. Baines, Phys. Rev. Lett. **98**, 077204 (2007).
[33] A. Yaouanc, P. Dalmas de Réotier, A. Bertin, C. Marin, E. Lhotel, A. Amato, and C. Baines, Phys. Rev. B **91**, 104427 (2015).
[34] A. Keren, P. Mendels, I. A. Campbell, and J. Lord, Phys. Rev. Lett. **77**, 1386 (1996).
[35] K. Ishida, D. E. MacLaughlin, B.-L. Young, K. Okamoto, Y. Kawasaki, Y. Kitaoka, G. J. Nieuwenhuys, R. H. Heffner, O. O. Bernal, W. Higemoto, A. Koda, R. Kadono, O. Trovarelli, C. Geibel, and F. Steglich, Phys. Rev. B **68**, 184401 (2003).
[36] D. E. MacLaughlin, R. H. Heffner, O. O. Bernal, K. Ishida, J. E. Sonier, G. J. Nieuwenhuys, M. B. Maple, and G. R. Stewart, J. Phys.: Condens. Matter **16**, S4479 (2004).
[37] D. T. Adroja, A. D. Hillier, J.-G. Park, W. Kockelmann, K. A. McEwen, B. D. Rainford, K.-H. Jang, C. Geibel, and T. Takabatake, Phys. Rev. B **78**, 014412 (2008).
[38] S. Lausberg, J. Spehling, A. Steppke, A. Jesche, H. Luetkens, A. Amato, C. Baines, C. Krellner, M. Brando, C. Geibel, H.-H. Klauss, and F. Steglich, Phys. Rev. Lett. **109**, 216402 (2012).
[39] R. Sarkar, J. Spehling, P. Materne, H. Luetkens, C. Baines, M. Brando, C. Krellner, and H.-H. Klauss, Phys. Rev. B **95**, 121111(R) (2017).
[40] R. Kubo and T. Toyabe, in *Magnetic Resonance and Relaxation*, edited by R. Blinc (North-Holland, Amsterdam, 1967), p. 810.
[41] S. Holenstein, U. Pachmayr, Z. Guguchia, S. Kamusella, R. Khasanov, A. Amato, C. Baines, H.-H. Klauss, E. Morenzoni, D. Johrendt, and H. Luetkens, Phys. Rev. B **93**, 140506(R) (2016).
[42] E. Wiesenmayer, H. Luetkens, G. Pascua, R. Khasanov, A. Amato, H. Potts, B. Banusch, H.-H. Klauss, and D. Johrendt, Phys. Rev. Lett. **107**, 237001 (2011).
[43] C. Bernhard, C. N. Wang, L. Nuccio, L. Schulz, O. Zaharko, J. Larsen, C. Aristizabal, M. Willis, A. J. Drew, G. D. Varma, T. Wolf, and C. Niedermayer, Phys. Rev. B **86**, 184509 (2012).
[44] T. Goltz, V. Zinth, D. Johrendt, H. Rosner, G. Pascua, H. Luetkens, P. Materne, and H.-H. Klauss, Phys. Rev. B **89**, 144511 (2014).
[45] P. Materne, S. Kamusella, R. Sarkar, T. Goltz, J. Spehling, H. Maeter, L. Harnagea, S. Wurmehl, B. Büchner, H. Luetkens, C. Timm, and H.-H. Klauss, Phys. Rev. B **92**, 134511 (2015).
[46] M. Bendele, A. Amato, K. Conder, M. Elender, H. Keller, H.-H. Klauss, H. Luetkens, E. Pomjakushina, A. Raselli, and R. Khasanov, Phys. Rev. Lett. **104**, 087003 (2010).
[47] T. Vojta, J. Phys. A: Math. Gen. **39**, R143 (2006).